Dalton Transactions

COMMUNICATION

View Article Online
View Journal | View Issue

Cite this: *Dalton Trans.*, 2014, **43**, 394

Received 31st July 2013,
Accepted 26th September 2013

DOI: 10.1039/c3dt52072b

www.rsc.org/dalton

Effect of ligand substituent on the reactivity of Ni(II) complexes towards oxygen†‡

Samir Ghorai and Chandan Mukherjee*

Two radical-containing Ni(II) complexes having either parent salicylidene (complex 1) or 3,5-di-*tert*-butylsalicylidene (complex 2) in the ligand backbone were synthesized. Complex 2 underwent ligand centered C–H activation by aerial oxygen, forming the corresponding amide complex (2a). The UV-Vis/NIR spectral changes upon purging of molecular oxygen to 2 in CH_2Cl_2, along with ESI-MS analysis indicated the generation of Ni–oxygen/dioxygen species as the intermediate(s) for the amide formation. Interestingly, non-participation of the ligand centered π-radical in the oxidation process was observed.

Metal-oxo units have been proposed as active intermediates for several enzymatic and biomimetic C–H bond activation reactions.[1] Since then, transition metal mediated dioxygen activation as well as the characterization of metal-oxo intermediates have drawn considerable attention from both chemists and biologists. Cu-, Co-, and Fe-based metalloenzymes[2] are well known for their oxygen activation, while Ni-based metalloenzymes are very rare.[1a] This could be due to the thermodynamically less favorable oxidation of Ni(II) by molecular oxygen, due to its higher oxidation state.[1a] However, electron rich ligands bound to the Ni(II) centre have been found to favor the Ni center oxidation process by decreasing the oxidation potential, and consequently Ni could be found in its higher oxidation state. For instance, Ni peptide complexes where the Ni center is bound to an amide ligand favor the oxidation of Ni(II) to Ni(III) under air.[3]

In continuation of our ongoing research in understanding the effect of substituents on the reactivity of metal complexes,[4] we have synthesized two new ligands, $H_3Sami^{Mixed(H)}$ and $H_3Sami^{Mixed(tBu)}$, composed of both redox active aminophenol (a change in its oxidation state is favored in the presence of a metal ion and oxygen) and redox inactive (a change in its oxidation state is not favored in the presence of a metal ion and oxygen) salicylidene compartments connected *via* a benzyl linker (Scheme 1). The ligands differ from each other by the presence of *tert*-butyl groups at the 3,5-positions of the salicylidene unit in $[(H_3Sami^{Mixed(tBu)})]$.

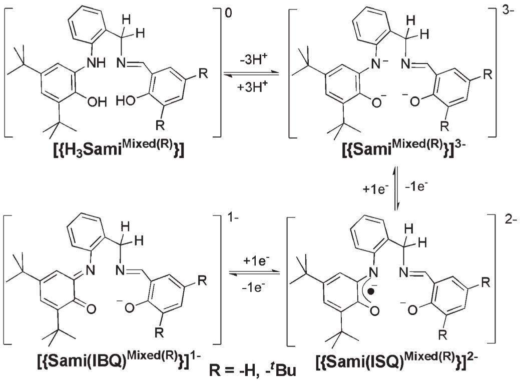

Scheme 1 A schematic representation of the ligands and their different redox states. ISQ and IBQ stand for the iminobenzosemiquinone and iminobenzoquinone forms of the ligand, respectively.

Herein, we report the synthesis of ligands $[(H_3Sami^{Mixed(tBu)})]$ and $[(H_3Sami^{Mixed(H)})]$, and their corresponding Ni(II) complexes. Interestingly, we have observed a remarkable substituent dependent reactivity of the Ni complexes with molecular oxygen. Non-participation of the ligand centered π-radical of the Ni–oxygen/dioxygen intermediate was also observed and reported here.

A schematic diagram for the synthesis of ligands $H_3Sami^{Mixed(H)}$, $H_3Sami^{Mixed(tBu)}$, and the corresponding Ni complexes **1** and **2** is shown in Scheme 2. The reaction between 1 : 1 2-aminobenzonitrile and 3,5-di-*tert*-butylcatechol in the presence of Et_3N provided H_2Sami^{CN} in 72% yield. Further reduction of the bidentate ligand using $LiAlH_4$ gave **A** in 70%

Department of Chemistry, Indian Institute of Technology Guwahati, Guwahati, 781039 Assam, India. E-mail: cmukherjee@iitg.ernet.in; Fax: (+)91-361-258-2349; Tel: (+)91-361-258-2327

† Dedicated to Dr Eckhard Bill on the occasion of his 60th birthday.

‡ Electronic supplementary information (ESI) available: Experimental procedures, characterization data of $H_3Sami^{Mixed(R)}$, **1**, **2**, and **2a**, including IR, mass spectra, ORTEP plots, and X-band EPR spectra. Crystallographic structural parameters, and crystallographic information file of $H_3Sami^{Mixed(H)}$, **1**, **2**, and **2a**. CCDC 951779–951782. For ESI and crystallographic data in CIF or other electronic format, see DOI: 10.1039/c3dt52072b

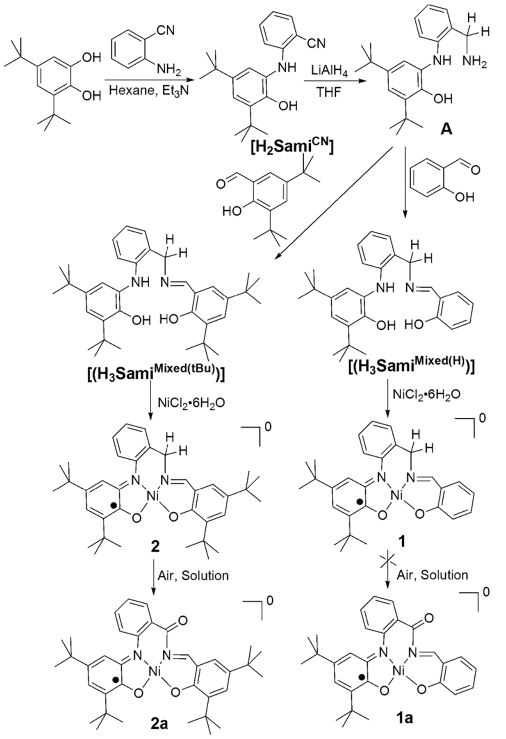

Scheme 2 A schematic representation of the ligands and the formation pathways of the corresponding Ni complexes.

yield. The condensation of equimolar amounts of salicylaldehyde and **A** in ethanol provided ligand $\mathrm{H_3Sami^{Mixed(H)}}$ in 70% yield. The ligand $\mathrm{H_3Sami^{Mixed(\mathit{t}Bu)}}$ was synthesized *in situ* by a 1 : 1 condensation of **A** with 3,5-di-*tert*-butylsalicylaldehyde in CH_3CN under reflux. The addition of $NiCl_2 \cdot 6H_2O$ to $\mathrm{H_3Sami^{Mixed(H)}}$ or to the *in situ* generated ligand $\mathrm{H_3Sami^{Mixed(\mathit{t}Bu)}}$ provided the corresponding complexes **1** and **2** in 51% and 40% yield, respectively. Both complexes were stable under air in the solid state. However, complex **2** changed gradually to complex **2a** when in solution.

Single crystal X-ray diffraction measurements for ligand $\mathrm{H_3Sami^{Mixed(H)}}$, complex **1**, complex **2**, and complex **2a** were performed at 296(2) K. Ligand $\mathrm{H_3Sami^{Mixed(H)}}$ crystallized in the triclinic space group $P\bar{1}$. The asymmetric ligand was comprised of three different kinds of C_6 aryl ring. The C–C bond distances of the C_6 aryl rings can be taken into consideration when assigning the oxidation state of the ligand. In the fully reduced form, the C–C bond distances in the C_6 aryl ring are all 1.39 ± 0.01 Å.[5,6] In the case of the one-electron oxidized iminobenzosemiquinone (ISQ) or two-electron oxidized iminobenzoquinone (IBQ) forms of the ligand (Scheme 1), discrete alternative short and long C–C bond distances (*i.e.* a quinoid-type distortion) in the C_6 aryl ring are expected.[5] Furthermore, in the ISQ form, the C_{Ph}–N_{Ph} and C_{Ph}–O_{Ph} (C_{Ph}, N_{Ph}, and O_{Ph} stand for the phenyl carbon atom, N, and O atom attached to the phenyl ring, respectively) bond distances are 1.35 ± 01 Å and 1.30 ± 0.01 Å, respectively.[5] These bond distances are in between single bond and double bond character, and correspond to the π-radical form of the organic moiety. In ligand $\mathrm{H_3Sami^{Mixed(H)}}$ the C–C bond distances of the 3,5-di-*tert*-butyl-containing aminophenol unit were in range of 1.380(5)–1.400(5) Å (Table 2, S14‡). The C1–N1 = 1.435(5) and C2–O1 = 1.375(5) Å bond distances along with the C–C bond distances indicated the fully reduced form of the aryl ring. The C14–N2 = 1.275(4) Å bond distance indicated its double bond character and the C20–O2 = 1.355(3) Å bond distance was in accord with the phenolic C–O bond distance.[6] The C–C bond distances of the other two C_6 rings were found to be in the range of 1.366(4)–1.402(4) Å with no quinoid-type distortion. Hence, the ligand was in its fully reduced form with the benzyl group bridging between an aminophenol and a salicylidene unit.

All of the complexes were neutral. Complex **1** and complex **2** crystallized in the monoclinic space groups $P2_1/a$ and $C2_1/c1$, respectively, while complex **2a** crystallized in the orthorhombic space group $P2_12_12_1$. The molecular structures are shown in Fig. 1. Selected bond distances and bond angles are given in Table 2 (S14–S15‡).

All of the C–C bond distances of the *tert*-butyl-containing C_6 aryl rings (amidophenolate unit) in the complexes were not within 1.39 ± 01 Å range, rather, a quinoid type distortion was observed (Table 2, S14–S15‡). Furthermore, the C1–N1 = 1.364(6) [**1**], 1.371(4) [**2**], 1.380(5) [**2a**] Å and C2–O1 = 1.293(8) [**1**], 1.310(3) [**2**], 1.305(5) [**2a**] Å (parentheses correspond to the respective complex) bond distances were in between those of their single bond and double bond values. There was shortening in the C20–O2 and C14–C15 bonds, and elongation in the C14–N2 bond, on going from free ligand to **1** or **2** (Table 2, S14–S15‡). These bond distance changes were mainly due to delocalization of the phenolate^{1-} charge over the O2–O20–C15–C14–N2 unit. The shortening and elongation of these bond distances in **2a** were more pronounced due to the increase of delocalization of the charge over the molecule *via* the newly formed amide unit. This type of shortening and elongation is common in salen complexes where the salicylidene unit is in its fully reduced form.[6] Hence, in the complexes, the amidophenolate part of the ligand was found to be in its one-electron oxidized ISQ form and no oxidation in the salen unit was observed.

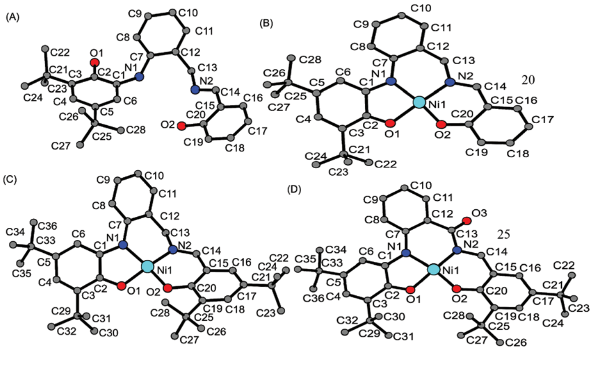

Fig. 1 Ball and stick representation of the (A) $\mathrm{H_3Sami^{Mixed(H)}}$, (B) **1**, (C) **2**, and (D) **2a** molecular structures. Hydrogen atoms are omitted for clarity.

In the complexes, the central Ni1 atom was coordinated by two N and two O atoms. The Ni1–O1, Ni1–N1 and Ni1–N2 bond distances were almost equal for both complexes, and found to be within the 1.86 ± 0.01 Å range. These bond distances were in accord with the +II oxidation state of the Ni center.[5b,c,6c,d] Interestingly, the Ni1–O2 bond distance was ~0.02 Å shorter in **2** compared to in **1**, indicating the higher covalency of the bond caused by the presence of the electron donating *tert*-butyl substituent at the 3,5-positions of the parent salicylidene unit. This difference in covalency seemed to be responsible for the observed difference in reactivity under air between **1** and **2**. A higher electron density at the Ni(II) center *via* PhO^- in **2** might facilitate the required stabilization of Ni to its higher oxidation state,[1b,7] and hence the oxygenation reaction.

A detailed solid-state structural comparison was performed and the parameters are given in Table 1 (S13‡). The Ni atom in **1** was observed to be almost planar with respect to both the **P** and **R** planes, while that in **2** was 0.30 Å below and 0.34 Å above the **P** and **R** planes, respectively. Furthermore, it was found that the position of the central Ni atom relative to the plane passing through the salicylidene unit differed remarkably (0.01 Å towards the benzyl carbon atom for **1** and 0.3 Å away from the benzyl carbon atom for **2**). These positional differences of the Ni(II) center seemed to facilitate formation of the oxygen–metal center adduct.

The X-band EPR spectra of **1**, **2**, and **2a** (Fig. 9, S8‡) displayed isotopic resonance signals at $g = 2.003$ (**1**), $g = 2.005$ (**2**) and $g = 2.002$ (**2a**) (parentheses indicate the complex). Thus, the neutral complexes can be best described as Ni(II)-mono(iminobenzosemiquinone) complexes, *i.e.* Ni(II) coordinated to a π-radical anion.

A CH_2Cl_2 solution of **2** was continuously purged with oxygen gas and time-dependent UV-Vis/NIR spectra were simultaneously recorded (Fig. 2). A gradual and regular increase in the absorption band (dotted lines) at ~652 nm was observed until 70 min. Noticeably, the band at ~835 nm, known as a marker of π-radical character,[5c] showed little change in absorption ($\varepsilon = 5000\ M^{-1}\ cm^{-1}$). This confirmed no reaction and/or participation of the ligand centered π-radical [**2**, ~835 nm (ε, $5500\ M^{-1}\ cm^{-1}$)]. The generation of the band at ~652 nm was related to the formation of diamagnetic species (28%) as evidenced by the decrease of the EPR signal (Fig. 13, S11‡). After 70 min, the band at ~652 nm gradually decreased with the increase of the product marking band at ~485 nm. This increase was related to the increase of the EPR signal (Fig. 13, S11‡).

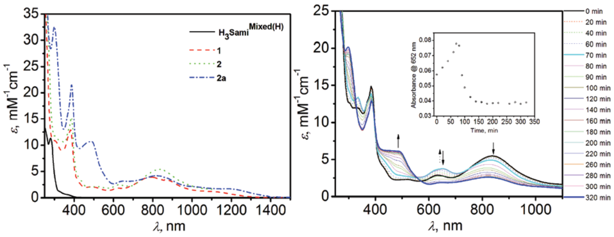

Fig. 2 UV-Vis/NIR spectra of $H_3Sami^{Mixed(H)}$, **1**, **2**, and **2a** (left). Time-dependent UV-vis/NIR spectral changes of **2** at RT in CH_2Cl_2 in the presence of molecular oxygen (right).

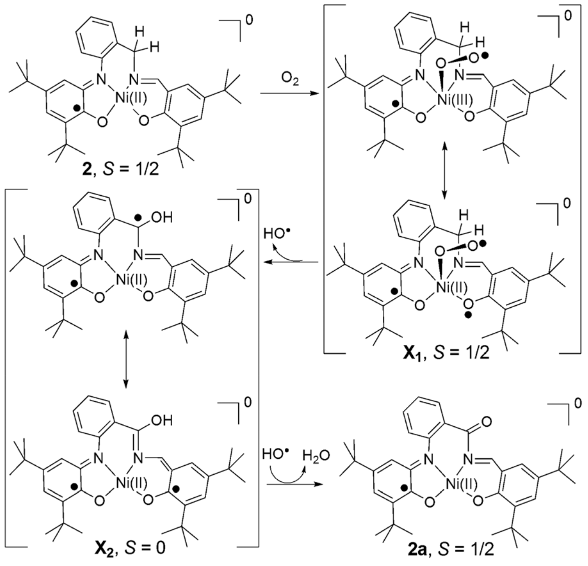

Scheme 3 A mechanistic proposal for the aerial oxidation of **2** to **2a**.

Ni(II) or Ni(III)-superoxo, -peroxo, -hydroperoxo, -oxide, and -hydroxo species do not give rise to a strong absorption band at ~652 nm.[8] Moreover, the addition of *m*CPBA (1 equiv.) to the CH_2Cl_2 solution of **2** gave rise to similar changes in the UV-Vis/NIR spectral features (Fig. 14, S12‡) as air did. Therefore, the species showing absorption at ~652 nm were not the corresponding -superoxo, -peroxo, or -hydroperoxo species. Herein, the band at ~652 nm was attributed to the generation of a diamagnetic species $\mathbf{X_2}$, having a delocalizing radical[9] at the benzyl position (Scheme 3).

The ESI (positive mode) mass spectrum of the reaction mixture (**2** + molecular oxygen) at 75 min showed peaks at $m/z = 613.30$ and $m/z = 630.30$, in addition to the molecular mass peaks for **2** and **2a** (Fig. 4, S8‡). The $m/z = 613.27$ peak and its isotope distribution pattern correspond to a $[\{(\mathbf{2} - H) + O\} + H]^+$ species, *i.e.* $[\mathbf{X_2} + H]^+$, while the $m/z = 630.26$ peak represents a $[\{\mathbf{2} + OO\} + H]^+$ unit, *i.e.* $[\mathbf{X_1} + H]^+$, a dioxygen–**2** adduct (Fig. 15, S12‡). When the reaction was carried out with $^{18}O_2$, the reaction solution exhibited ion peaks at $m/z = 615.29$ and 613.34. These peaks corresponded to $[\mathbf{2} + {}^{18}O]^+$ and [**2a** (with one ^{18}O)] species with the expected isotope distribution pattern (Fig. 14, S12‡). This labeling experiment confirmed the incorporation of one oxygen atom from molecular oxygen into **2a**, in addition to the transient intermediate (Fig. 15, S12‡). Considering the above experimental (UV-Vis/NIR, X-band EPR, MS) observations, the oxidation process seemed to proceed *via* the route presented in Scheme 3.

Conclusions

To conclude, two asymmetric ligands and their corresponding Ni(II) complexes (**1** and **2**) coordinated to a π-radical anion were synthesized. Among them, **2** underwent ligand centered C–H bond activation, and consequently a *keto* (C=O) bond formation by reaction with air as the sole oxidant. It was found from X-ray crystallography that the position of the Ni center above the salicylidene plane, and its higher covalency were necessary to activate Ni(II) towards reaction with air. In contrast to **1**, the *tert*-butyl groups present at the salicylidene unit in **2** stabilize the generated radical-containing transient species in its delocalized form, thus favoring the oxidation process.

In general, Ni-oxo, -hydroxo, -peroxo, and -superoxo species are generated either through reaction of oxygen with low-valent Ni(0/I) complexes, or by reaction of Ni(II) complexes with activated oxygen from oxygen releasing sources {*e.g.* hydrogen peroxide (H_2O_2), *meta*-chloroperbenzoic acid (*m*CPBA), *etc.*},[8] whereas complex **2** was converted to its oxygenated product only by reaction with air. This is a very rare example.[8e] Further investigations on the reaction mechanism and the effects of substitution by employing different substituents at the salen unit are ongoing, and our findings might provide Ni(II) complexes as catalysts for aerial oxidation and/or oxygenation *via* C–H activation.

CCDC 951782 [$H_3Sami^{Mixed(H)}$], 951779 [**1**], 951780 [**2**], and 951781 [**2a**] contain the supplementary crystallographic data for this paper.

Acknowledgements

This project was funded by DST (SR/FT/CS-86/2011). SG thanks UGC (India) for doctoral fellowship. Dr T. K. Paine and Dr A. Patra are thankfully acknowledged for their help in general.

Notes and references

1 (*a*) M. T. K. Emmons and C. G. Riordan, *Acc. Chem. Res.*, 2007, **40**, 618; (*b*) S. Yao and M. Driess, *Acc. Chem. Res.*, 2012, **45**, 276.

2 (*a*) E. Y. Tshuva and S. J. Lippard, *Chem. Rev.*, 2004, **104**, 987; (*b*) E. I. Solomon, T. C. Brunold, M. I. Davis, J. N. Kemsley, S.-K. Lee, N. Lehnert, F. Neese, A. J. Skulan, Y.-S. Yang and J. Zhou, *Chem. Rev.*, 2000, **100**, 235; (*c*) M. Akita and S. Hikichi, *Bull. Chem. Soc. Jpn.*, 2002, **75**, 1657; (*d*) N. Kitajima and Y. Moro-oka, *Chem. Rev.*, 1994, **94**, 737; (*e*) M. A. Kopf and K. D. Karlin, in *Biomimetic Oxidations*, ed. B. Muenier, Imperial College Press, London, U.K., 2000, ch. 7; (*f*) L. Q. Hatcher and K. D. Karlin, *J. Biol. Inorg. Chem.*, 2004, **9**, 669.

3 (*a*) W. Bal, M. I. Djuran, D. W. Margerum, T. Edward, J. Gray, M. A. Mazid, R. T. Tom, E. Nieboer and P. J. Sadler, *J. Chem. Soc., Chem. Commun.*, 1994, 1889; (*b*) M. Suzuki, *Acc. Chem. Res.*, 2007, **40**, 609.

4 S. Ghorai and C. Mukherjee, *Chem. Commun.*, 2012, 10180.

5 (*a*) A. L. Smith, K. I. Hardcastle and J. D. Soper, *J. Am. Chem. Soc.*, 2010, **132**, 14358; (*b*) C. Mukherjee, T. Weyhermüller, E. Bothe and P. Chaudhuri, *Inorg. Chem.*, 2008, **47**, 2740; (*c*) C. Mukherjee, T. Weyhermüller, E. Bothe and P. Chaudhuri, *Inorg. Chem.*, 2008, **47**, 11620.

6 (*a*) C. Mukherjee, A. Stmmler, H. Bögge and T. Glaser, *Inorg. Chem.*, 2009, **48**, 9476; (*b*) C. Mukherjee, A. Stmmler, H. Bögge and T. Glaser, *Chem.–Eur. J.*, 2010, 10137; (*c*) T. Glaser, M. Heidemeier, R. Föhlich, P. Hildebrandt, E. Bothe and E. Bill, *Inorg. Chem.*, 2005, **44**, 5467; (*d*) O. Rotthaus, O. Jarjayes, F. Thomas, C. Philouze, C. P. D. Valle, E. S. Aman and J. L. Pierre, *Chem.–Eur. J.*, 2006, **12**, 2293.

7 (*a*) S. Otsuka, A. Nakamura and Y. Tatsuno, *J. Am. Chem. Soc.*, 1969, **91**, 6994; (*b*) S. Sripothongnak, N. Barone and C. J. Ziegler, *Chem. Commun.*, 2009, 4584.

8 (*a*) T. D. Manuel and J.-U. Rohde, *J. Am. Chem. Soc.*, 2009, **131**, 15582; (*b*) F. F. Pfaff, F. Heims, S. Kundu and K. Ray, *Chem. Commun.*, 2012, 3730; (*c*) A. Company, S. Yao, K. Ray and M. Driess, *Chem.–Eur. J.*, 2010, **16**, 9669; (*d*) J. Cho, R. Sarangi, J. Annaraj, S. Y. Kim, M. Kubo, T. Ogura, E. I. Solomon and W. Nam, *Nat. Chem.*, 2009, **1**, 568; (*e*) B. Bag, M. Mondal, G. Rosair and S. Mitra, *Chem. Commun.*, 2000, 1729.

9 (*a*) J. Seth, V. Palaniappan and D. F. Bocian, *Inorg. Chem.*, 1995, **34**, 2201; (*b*) D. Chang, T. Malinski, A. Ulman and K. M. Kadish, *Inorg. Chem.*, 1984, **23**, 817.